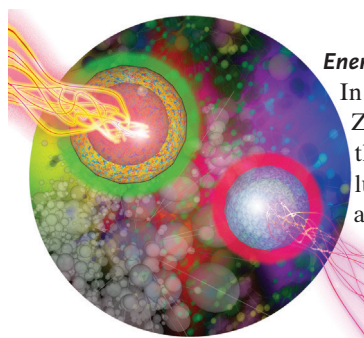
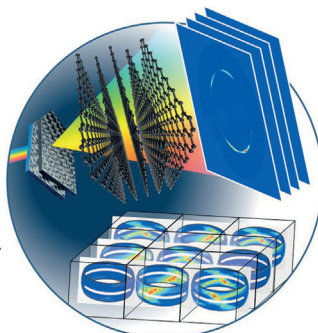


... of Norse mythology that encircled Midgard—arylethynyl oligomers envelop their guests with halogen bonds. In their Communication on page 12398 ff., O. B. Berryman et al. present the first halogen-bond-induced triple helicate to encapsulate iodide in solution and the solid state. Strong and linear halogen bonds promote this intricate and robust self-assembly. Garron Hale (Univ. of Oregon) is gratefully acknowledged for assisting with preparation of the cover artwork.

## Crystallographic Texture

H. C. Lichtenegger et al. describe in their Communication on page 12190 ff. a method to determine crystallographic texture. The method is based on energy-dispersive Laue diffraction and enables 3D information to be obtained without sample rotation.

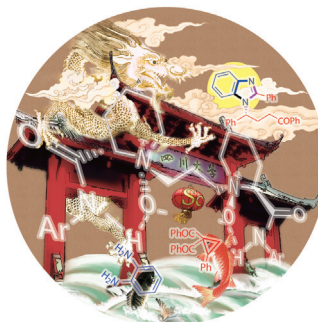


## Energy Transfer

In their Communication on page 12356 ff., B. Zhou, Q. Y. Zhang, Y. H. Tsang et al. demonstrate the realization of both up- and down-conversion luminescence of lanthanides by using gadolinium as energy donor in a core-shell nanostructure.

## Asymmetric Synthesis

The first asymmetric ring-opening/cyclization/retro-Mannich reaction of cyclopropyl ketones with aryl-1,2-diamines is described by X. M. Feng, X. H. Liu et al. in their Communication on page 12228 ff.



## How to contact us:

### Editorial Office:

E-mail: [angewandte@wiley-vch.de](mailto:angewandte@wiley-vch.de)

Fax: (+49) 62 01-606-331

Telephone: (+49) 62 01-606-315

### Reprints, E-Prints, Posters, Calendars:

Carmen Leitner

E-mail: [chem-reprints@wiley-vch.de](mailto:chem-reprints@wiley-vch.de)

Fax: (+49) 62 01-606-331

Telephone: (+49) 62 01-606-327

### Copyright Permission:

Bettina Loycke

E-mail: [rights-and-licences@wiley-vch.de](mailto:rights-and-licences@wiley-vch.de)

Fax: (+49) 62 01-606-332

Telephone: (+49) 62 01-606-280

### Online Open:

Margitta Schmitt

E-mail: [angewandte@wiley-vch.de](mailto:angewandte@wiley-vch.de)

Fax: (+49) 62 01-606-331

Telephone: (+49) 62 01-606-315

### Subscriptions:

[www.wileycustomerhelp.com](http://www.wileycustomerhelp.com)

Fax: (+49) 62 01-606-184

Telephone: 0800 1800536 (Germany only)  
+44(0) 1865476721 (all other countries)

### Advertising:

Marion Schulz

E-mail: [mschulz@wiley-vch.de](mailto:mschulz@wiley-vch.de)

Fax: (+49) 62 01-606-550

Telephone: (+49) 62 01-606-565

### Courier Services:

Boschstrasse 12, 69469 Weinheim

### Regular Mail:

Postfach 101161, 69451 Weinheim

Angewandte Chemie International Edition is a journal of the Gesellschaft Deutscher Chemiker (GDCh), the largest chemistry-related scientific society in continental Europe. Information on the various activities and services of the GDCh, for example, cheaper subscription to *Angewandte Chemie International Edition*, as well as applications for membership can be found at [www.gdch.de](http://www.gdch.de) or can be requested from GDCh, Postfach 900440, D-60444 Frankfurt am Main, Germany.

GDCh

GESELLSCHAFT  
DEUTSCHER CHEMIKER

Get the **Angewandte App**  
International Edition



Enjoy Easy Browsing and a New Reading Experience on Your Smartphone or Tablet

- Keep up to date with the latest articles in Early View.
- Download new weekly issues automatically when they are published.
- Read new or favorite articles anytime, anywhere.

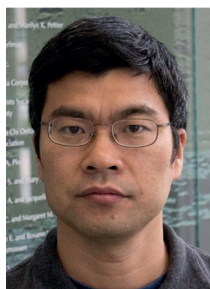


## Service

Spotlight on Angewandte's Sister Journals

12138 – 12141

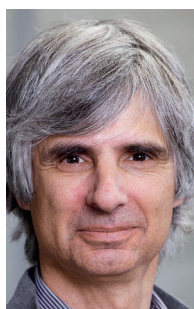
## Author Profile



*"If I were not a scientist, I would be a chef.  
My greatest achievement has been volunteering in my  
son's kindergarten class for nearly one year. ..."*  
This and more about Weiping Tang can be found on  
page 12142.

Weiping Tang \_\_\_\_\_ 12142

## News



B. H. Meier



H.-P. Steinrück



H. Braunschweig



W. Kutzelnigg

New Members of the Deutsche  
Akademie der Naturforscher  
Leopoldina: B. H. Meier and  
H.-P. Steinrück \_\_\_\_\_ 12143

Alfred Stock Memorial Prize:  
H. Braunschweig \_\_\_\_\_ 12143

Erich Hückel Prize:  
W. Kutzelnigg \_\_\_\_\_ 12143

## Books

Handbook of Bibliometric Indicators

Roberto Todeschini, Alberto Baccini

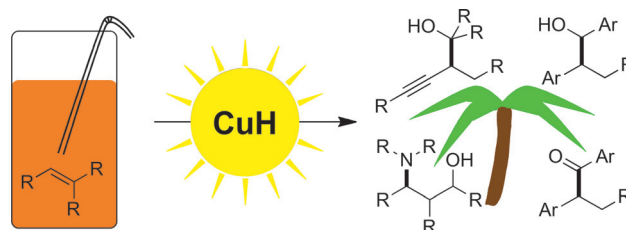
reviewed by J. Reedijk\* \_\_\_\_\_ 12144

## Highlights

## Asymmetric Catalysis

J. Mohr, M. Oestreich\* — 12148–12149

Balancing C=C Functionalization and C=O Reduction in Cu–H Catalysis



**Coppercabana:** The copper(I) hydride catalyzed functionalization of unactivated alkenes has been shown to be compatible with conventional carbonyl reduction. Through the combination of both path-

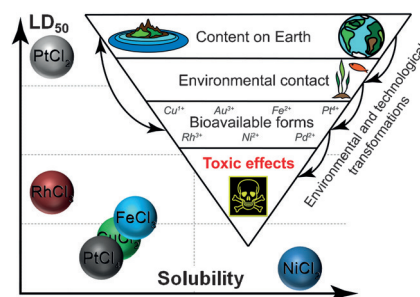
ways or complete suppression of C=O reduction in favor of C=C functionalization, methods for the stereoselective synthesis of a variety of chiral molecules have been developed.

## Minireviews

## Sustainable Chemistry

K. S. Egorova,  
V. P. Ananikov\* — 12150–12162Which Metals are Green for Catalysis?  
Comparison of the Toxicities of Ni, Cu, Fe,  
Pd, Pt, Rh, and Au Salts

**Heavy weights versus the light weights:** A comparison of available data on biological activity of metals commonly used in catalysis suggests that the assumption of toxic heavy metals and benign lighter metals should be re-evaluated. The available experimental data are insufficient for accurate evaluation of biological activity of these metals. Therefore, without dedicated experimental measurements, toxicity should not be used as a “selling point” when describing new catalysts.

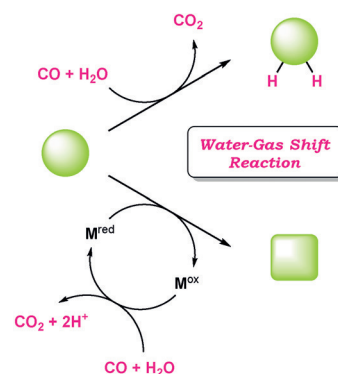


## Reviews

## Synthetic Methods

A. Ambrosi,  
S. E. Denmark\* — 12164–12189Harnessing the Power of the Water-Gas  
Shift Reaction for Organic Synthesis

**New directions for a classic:** In addition to its fundamental role in the production of hydrogen, the water-gas shift reaction has found application in a multitude of reductive transformations in organic synthesis. These include hydrogenation-type reactions, as well as catalytic, overall-reductive processes wherein the CO/H<sub>2</sub>O couple can act as the terminal reductant.



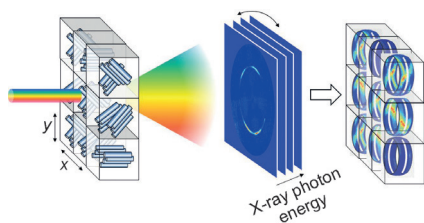
## For the USA and Canada:

ANGEWANDTE CHEMIE International Edition (ISSN 1433-7851) is published weekly by Wiley-VCH, PO Box 101161, 69451 Weinheim, Germany. US mailing agent: SPP, PO Box 437, Emigsville, PA 17318. Periodicals postage

paid at Emigsville, PA. US POSTMASTER: send address changes to *Angewandte Chemie*, John Wiley & Sons Inc., C/O The Sheridan Press, PO Box 465, Hanover, PA 17331. Annual subscription price for institutions: US\$ 16.862/14.051 (valid for print and electronic / print or

electronic delivery); for individuals who are personal members of a national chemical society prices are available on request. Postage and handling charges included. All prices are subject to local VAT/sales tax.





**In full view:** A new method to determine crystallographic texture based on energy-dispersive Laue diffraction exploits the curvature of the Ewald sphere to obtain 3D information in one shot without sample rotation, which opens up unprecedented spatial resolution. The principle was demonstrated on a complex carbon fiber system as well as the biomineralized exocuticle tissue of the American lobster.

## Communications

### Crystallographic Texture

T. A. Grünwald, H. Rennhofer, P. Tack, J. Garrevoet, D. Wermeille, P. Thompson, W. Bras, L. Vincze, H. C. Lichtenegger\* — 12190–12194

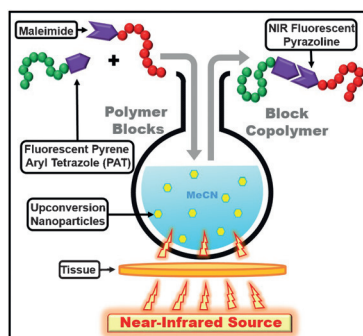
Photon Energy Becomes the Third Dimension in Crystallographic Texture Analysis



### Frontispiece



**Gently does it:** The first example of upconversion photoinduced coupling chemistry based on the established tetrazole–ene cycloaddition system induced by near-infrared light is introduced. The power of the technique, including tissue penetration, is demonstrated for small-molecule ligation, macromolecular end-group modification as well as polymer–polymer ligation.



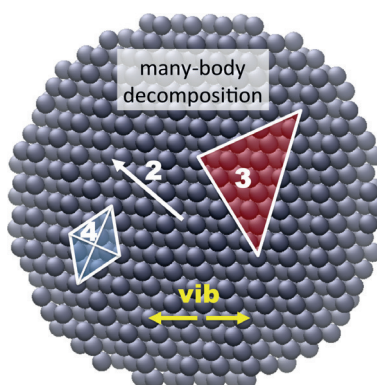
### Photochemistry

P. Lederhose, Z. Chen, R. Müller, J. P. Blinco,\* S. Wu,\* C. Barner-Kowollik\* — 12195–12199

Near-Infrared Photoinduced Coupling Reactions Assisted by Upconversion Nanoparticles



**Testing theory at the very limit:** The cohesive energy for solid argon is obtained from a many-body decomposition into static and dynamic contributions by application of relativistic coupled cluster theory. The deviation from experimental findings is in the  $\text{J mol}^{-1}$  range.

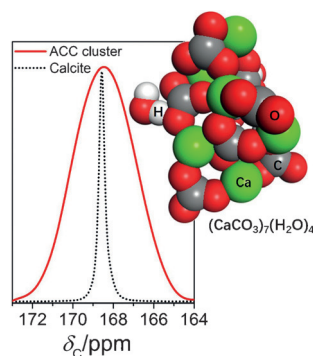


### Computational Chemistry

P. Schwerdtfeger,\* R. Tonner, G. E. Moyano, E. Pahl — 12200–12205

Towards J/mol Accuracy for the Cohesive Energy of Solid Argon

**Proto-calcite short-range order** was found in ligand-stabilized amorphous calcium carbonate clusters with a very small  $\text{CaCO}_3$  core 1.4 nm in diameter consisting of only seven  $\text{CaCO}_3$  units. This supports the notion of a structural link between prenucleation clusters and the postnucleation amorphous phase.



### Crystallization

S. T. Sun, D. M. Chevrier, P. Zhang, D. Gebauer,\* H. Cölfen\* — 12206–12209

Distinct Short-Range Order Is Inherent to Small Amorphous Calcium Carbonate Clusters (< 2 nm)





## Environmental Chemistry

F. Topuz,\* S. Singh, K. Albrecht,  
M. Möller, J. Groll\* — 12210–12213



DNA Nanogels To Snare Carcinogens:  
A Bioinspired Generic Approach with  
High Efficiency



**Take it away:** DNA nanogels were developed as a biomimetic scavenging agent by exploiting the generic complexation of DNA with polycyclic aromatic hydrocarbons (PAHs). Up to 720 µg of PAH per gram of DNA nanogel are taken up and

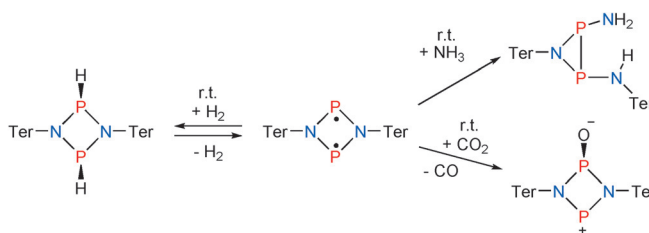
the uptake is rapid, reaching 50% loading after 15 minutes. Beyond PAHs, DNA nanogels may be useful for the generic removal of genotoxins from water, since most known molecules that strongly associate with DNA are mutagenic.

## Main-Group Chemistry

A. Hinz, A. Schulz,\*  
A. Villinger — 12214–12218



Metal-Free Activation of Hydrogen,  
Carbon Dioxide, and Ammonia by the  
Open-Shell Singlet Biradicaloid  
[P(μ-NTer)]<sub>2</sub>



**Don't wait for activation:** The singlet biradicaloid [P(μ-NTer)]<sub>2</sub> readily reacts with H<sub>2</sub>, CO<sub>2</sub>, or NH<sub>3</sub> at ambient temperature. The addition of H<sub>2</sub> is reversible whereas CO<sub>2</sub> is reduced to CO with

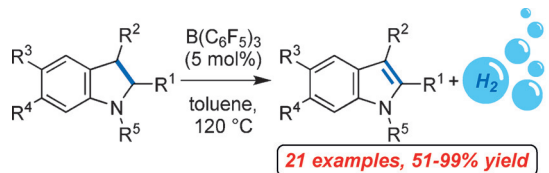
formation of “biradicaloid monoxide”. Activation of ammonia causes the P<sub>2</sub>N<sub>2</sub> scaffold to rearrange to give an azadi-phosphirine.

## Dehydrogenation

A. F. G. Maier, S. Tussing, T. Schneider,  
U. Flörke, Z.-W. Qu, S. Grimme,\*  
J. Paradies\* — 12219–12223



Frustrated Lewis Pair Catalyzed  
Dehydrogenative Oxidation of Indolines  
and Other Heterocycles



**The acceptorless dehydrogenation** of N-protected indolines and other heterocycles is catalyzed by frustrated Lewis pairs. Mechanistic as well as quantum-mechanical studies revealed the liberation

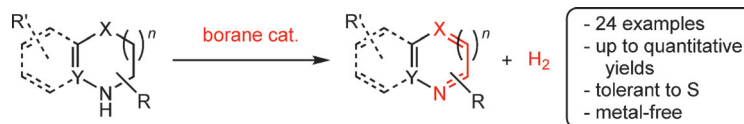
of molecular hydrogen to be the rate-determining step. The addition of a weaker Lewis acid as a hydride shuttle increased the reaction rate by a factor of 2.28.

## Heterocycles

M. Kojima, M. Kanai\* — 12224–12227

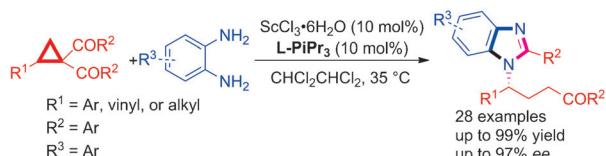


Tris(pentafluorophenyl)borane-Catalyzed  
Acceptorless Dehydrogenation of  
N-Heterocycles



**B-side of borane:** A metal-free acceptorless dehydrogenation of N-heterocycles was realized by using an electrophilic borane. This protocol affords synthetically important N-heteroarenes in high yield. The borane catalyst exhibits unprece-

dent chemoselectivity as it is tolerant to sulfur functionalities and demonstrates superior reactivity in the synthesis of benzothiazoles compared to the conventional metal-catalyzed methods.



**Scandalous Sc:** The title reaction proceeds in the presence of a chiral *N,N'*-dioxide/*Sc*<sup>III</sup> catalyst. A variety of benzimidazoles bearing chiral side chains were

obtained with excellent results. This method provides novel access to chiral benzimidazole-substituted amide and cycloheptene derivatives.

## Heterocycle Synthesis

Y. Xia, L. L. Lin, F. Z. Chang, Y. T. Liao, X. H. Liu,\* X. M. Feng\* — 12228 – 12232

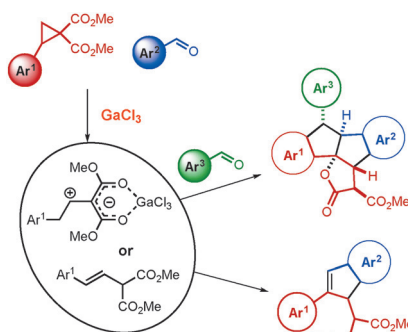
Asymmetric Ring Opening/Cyclization/Retro-Mannich Reaction of Cyclopropyl Ketones with Aryl 1,2-Diamines for the Synthesis of Benzimidazole Derivatives



Back Cover



**Old reagents, new products:** A new strategy for the cascade assembly of substituted indenenes and polycyclic lactones based on reactions of donor–acceptor cyclopropanes and styrylmalonates with aromatic aldehydes has been developed. Use of  $\text{GaCl}_3$  makes it possible to change the direction of the reaction and to perform the process in a multicomponent version (27 examples).



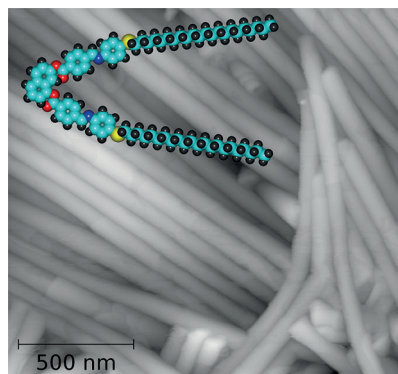
## Cascade Reactions

D. D. Borisov, R. A. Novikov, Y. V. Tomilov\* — 12233 – 12237

$\text{GaCl}_3$ -Mediated Reactions of Donor–Acceptor Cyclopropanes with Aromatic Aldehydes



**The lamellar crystal phase (*B*<sub>4</sub>)** made of acute-angle bent-core mesogens exhibits an unusual, highly porous sponge-like morphology. However, if grown in the presence of low-weight mesogenic molecules, the same crystal forms nanotubes with a very high aspect ratio.



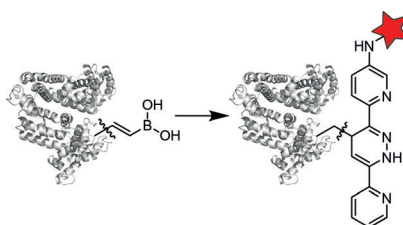
## Crystalline Phases

E. Gorecka,\* N. Vaupotič, A. Zep, D. Pociecha — 12238 – 12242

From Sponges to Nanotubes: A Change of Nanocrystal Morphology for Acute-Angle Bent-Core Molecules



**Bioorthogonal iEDDA reagents:** Vinylboronic acids (VBAs) were studied as non-strained, synthetically accessible, and water-soluble bioorthogonal reagents in the Carboni–Lindsey reaction with dipyrrolyl-*s*-tetrazines. The VBAs were shown to be biocompatible, non-toxic, and highly stable in aqueous media and cell lysate. Furthermore, VBAs were used orthogonally to the strain-promoted alkyne–azide cycloaddition for protein modification.



## Bioorthogonal Reactions

S. Eising, F. Lelivelt, K. M. Bonger\* — 12243 – 12247

Vinylboronic Acids as Fast Reacting, Synthetically Accessible, and Stable Bioorthogonal Reactants in the Carboni–Lindsey Reaction

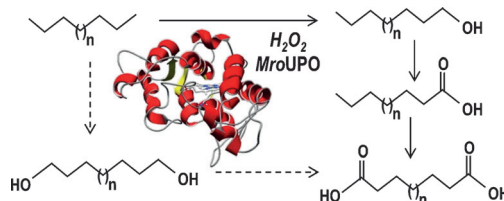


## Enzyme Catalysis

A. Olmedo, C. Aranda, J. C. del Río,  
J. Kiebitz, K. Scheibner, A. T. Martínez,  
A. Gutiérrez\* — 12248 – 12251



From Alkanes to Carboxylic Acids:  
Terminal Oxygenation by a Fungal  
Peroxxygenase



A **peroxxygenase** from the fungus *Marasmius rotula* was found to catalyze a cascade of mono- and diterminal oxygenation reactions of long-chain *n*-alkanes to carboxylic acids in the presence of  $H_2O_2$  as the sole cosubstrate (see scheme). This

peroxxygenase type has great advantages for the mild activation of alkanes, with its self-sufficient monooxygenase activity and its ability to hydroxylate the most unreactive terminal positions.

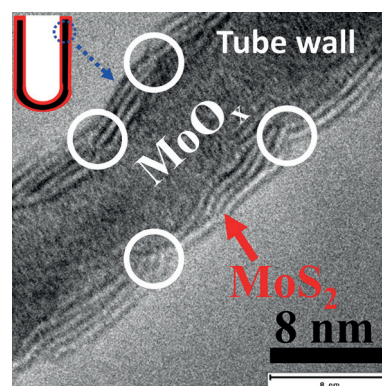
## Electrocatalysis

B. Jin, X. Zhou, L. Huang, M. Lickleder,  
M. Yang,\* P. Schmuki\* — 12252 – 12256



Aligned  $MoO_x/MoS_2$  Core-Shell  
Nanotubular Structures with a High  
Density of Reactive Sites Based on Self-  
Ordered Anodic Molybdenum Oxide  
Nanotubes

**Anodic molybdenum oxide** nanotube arrays were formed. These  $MoO_x$  nanotube layers can be converted into a  $MoO_x/MoS_2$  nanotubular core-shell structure with bent  $MoS_2$  nanosheets consisting of stacks of typically four S-Mo-S layer units, which are discordantly grown on the  $MoO_x$  substrate, exposing catalytically active end planes to the surrounding. These structures are highly promising for applications in electrocatalysis.

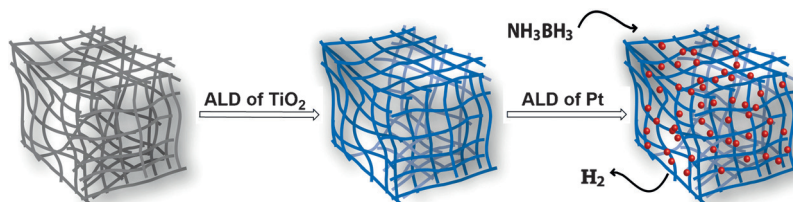


## 3D Nanomaterials

M. A. Khalily, H. Eren, S. Akbayrak,  
H. H. Susapto, N. Biyikli,\* S. Özkar,\*  
M. O. Guler\* — 12257 – 12261



Facile Synthesis of Three-Dimensional  
Pt- $TiO_2$  Nano-networks: A Highly Active  
Catalyst for the Hydrolytic Dehydro-  
genation of Ammonia-Borane



A **3D peptide nanofiber aerogel** was coated with  $TiO_2$  by atomic layer deposition (ALD) with angstrom-level thickness precision. This nano-network was further decorated with Pt nanoparticles (Pt NPs;

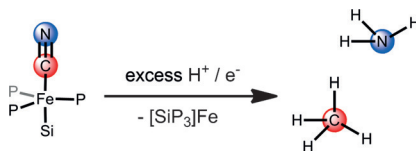
see picture; red) using ozone-assisted ALD. The 3D Pt- $TiO_2$  nano-network shows superior catalytic activity in hydrolysis of ammonia-borane, generating 3 equivalents of  $H_2$ .

## Nitrogen Fixation

J. Rittle, J. C. Peters\* — 12262 – 12265

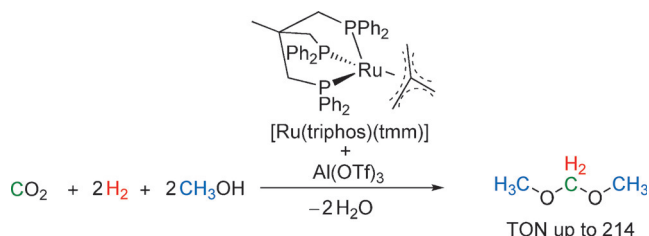


Proton-Coupled Reduction of an Iron  
Cyanide Complex to Methane and  
Ammonia



**Reductive cleavage of cyanide:** A trigonal bipyramidal iron cyanide complex is shown to evolve methane and ammonia upon exposure to proton and electron equivalents at low temperature (see picture). Terminally bound  $Fe(CNH)$  and  $Fe(CNH_2)$  complexes are characterized as possible intermediates in this  $CN^-$  cleavage reaction.





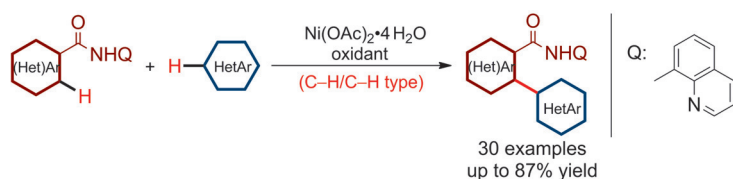
**Come together!** The molecular catalyst [Ru(triPhos)(tmm)] in combination with the Lewis acid Al(OTf)<sub>3</sub> enables the synthesis of dimethoxymethane from carbon dioxide, molecular hydrogen and methanol. This new catalytic reaction provides

the first synthetic example for the selective conversion of carbon dioxide and hydrogen into the formaldehyde oxidation level, thus opening access to new molecular structures using this important C<sub>1</sub> source.



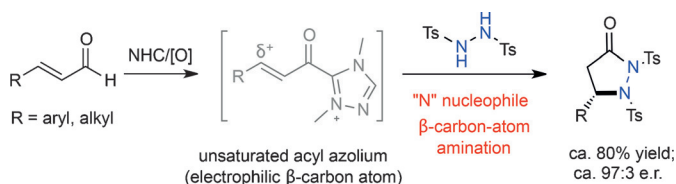
**All about efficiency:** The title reaction tolerates a variety of arylboronic acids and widely available difluoroalkyl bromides, and even the relatively inert substrate

chlorodifluoroacetate. The protocol provides a highly efficient method for the catalytic synthesis of difluoroalkylated compounds.



**An odd couple:** The title reaction with the aid of the 8-aminoquinoline group gives biheteroaryl structural motifs. The reaction exhibits high functional-group com-

patibility and broad substrate scope, and the silver oxidant can be recycled to reduce costs and waste.



**Focus on the β-C:** The aza-Michael addition of protected hydrazine to a catalytically generated unsaturated acyl azolium intermediate provides a highly efficient approach for enantioselective β-carbon-atom amination of enals. The heterocyclic

products, prepared by using this method, are common scaffolds found in bioactive molecules, and can be readily transformed into β<sup>3</sup>-amino-acid derivatives. NHC = N-heterocyclic carbene.

## CO<sub>2</sub> Utilization

K. Thenert, K. Beydoun, J. Wiesenthal, W. Leitner, J. Klankermayer\* 12266 – 12269

Ruthenium-Catalyzed Synthesis of Dialkoxymethane Ethers Utilizing Carbon Dioxide and Molecular Hydrogen



## Cross-Coupling

J.-W. Gu, Q.-Q. Min, L.-C. Yu, X. Zhang\* 12270 – 12274

Tandem Difluoroalkylation-Arylation of Enamides Catalyzed by Nickel



## Homogeneous Catalysis

Y. Cheng, Y. Wu, G. Tan, J. You\* 12275 – 12279

Nickel Catalysis Enables Oxidative C(sp<sup>2</sup>)–H/C(sp<sup>2</sup>)–H Cross-Coupling Reactions between Two Heteroarenes



## Heterocycle Synthesis

X. Wu, B. Liu, Y. Zhang, M. Jeret, H. Wang, P. Zheng, S. Yang,\* B.-A. Song, Y. R. Chi\* 12280 – 12284

Enantioselective Nucleophilic β-Carbon-Atom Amination of Enals: Carbene-Catalyzed Formal [3+2] Reactions



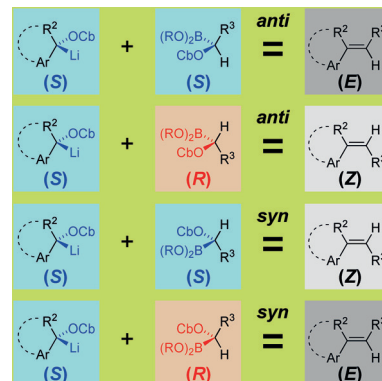
## Alkene Synthesis

Z. Wu, X. Sun, K. Potter, Y. Cao,  
L. N. Zakharov,  
P. R. Blakemore\* 12285 – 12289



Stereospecific Synthesis of Alkenes by  
Eliminative Cross-Coupling of  
Enantioenriched  $sp^3$ -Hybridized  
Carbenoids

**3D to 2D:** Stereochemical information encoded in a pair of scalemic carbenoid reagents controls the geometry of the alkene products formed by their eliminative cross-coupling. The configuration of the alkene is determined by the carbenoid stereochemical pairing (*like* or *unlike*) and the elimination mechanism (*syn* or *anti*), but not by the nature of the substituents.

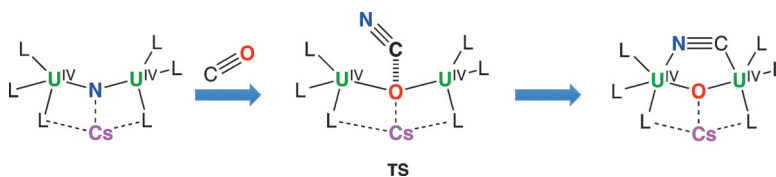


## CO Cleavage

M. Falcone, C. E. Kefalidis, R. Scopelliti,  
L. Maron,\* M. Mazzanti\* 12290 – 12294



Facile CO Cleavage by a Multimetallic  
 $CsU_2$  Nitride Complex



**The power of cooperation:** A heteropoly-metallic uranium nitride with a  $CsU^{IV}-N-U^{IV}$  core effected complete cleavage of the strong  $C\equiv O$  bond of carbon monoxide under ambient conditions (see scheme). The reaction led to the formation of a  $CN^-$

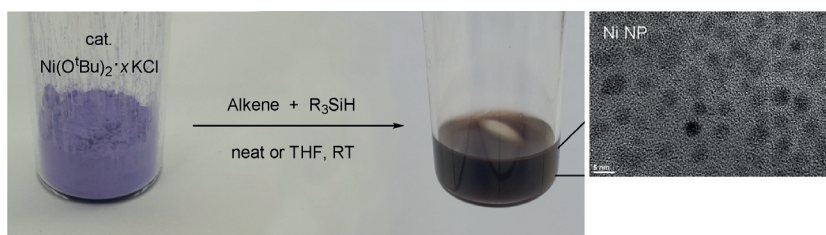
ligand, which could be alkylated readily to afford organic nitriles. The important role of multimetallic cooperativity in these reactions was identified by computation of the reaction mechanisms.

## Hydrosilylation

I. Buslov, F. Song,  
X. L. Hu\* 12295 – 12299



An Easily Accessed Nickel Nanoparticle  
Catalyst for Alkene Hydrosilylation with  
Tertiary Silanes



**A nickel nanoparticle catalyst** is an efficient and non-precious catalyst for alkene hydrosilylation with commercially relevant

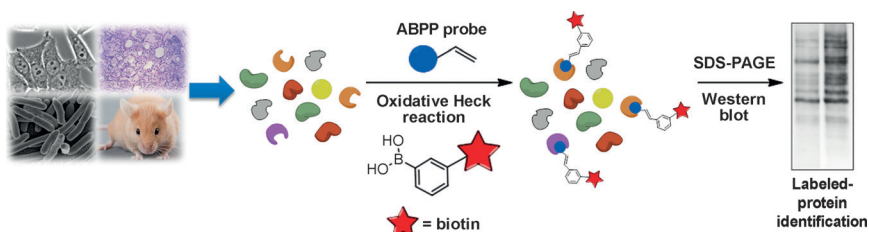
tertiary silanes. 28 examples of silanes were formed by this method.

## Enzyme Labeling

N. Eleftheriadis, S. A. Thee,  
M. R. H. Zwinderman, N. G. J. Leus,  
F. J. Dekker\* 12300 – 12305

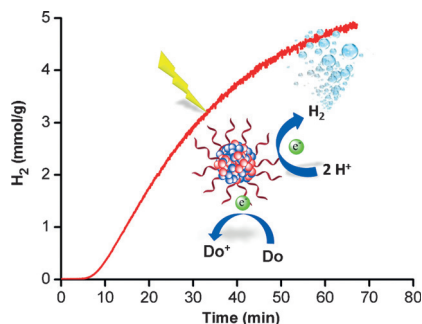


Activity-Based Probes for  
15-Lipoxygenase-1



**A villain meets its match:** An activity-based probe was developed for human 15-lipoxygenase-1 (15-LOX-1), which plays an important role in various diseases. The probe mimicked the natural enzyme substrate and was able to bind covalently to

the active enzyme. It included a terminal alkene as a chemical reporter for the bioorthogonal linkage of a detectable functionality by the oxidative Heck reaction (see scheme).



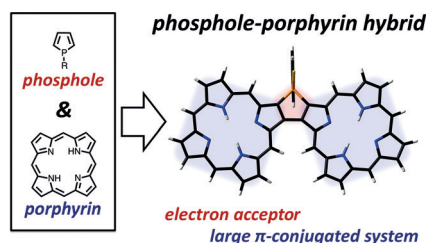
**Organic polymer dots** were used as a photocatalyst for visible-light-driven hydrogen generation for the first time and showed impressive activity with an initial hydrogen generation rate of  $8.3 \text{ mmol h}^{-1} \text{ g}^{-1}$  without the assistance of any co-catalysts. Do = donor.

### Photocatalysis

L. Wang, R. Fernández-Terán, L. Zhang, D. L. A. Fernandes, L. Tian, H. Chen, H. Tian\* — 12306–12310

Organic Polymer Dots as Photocatalysts for Visible Light-Driven Hydrogen Generation

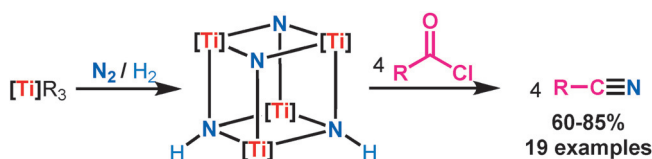
**A phosphole-fused porphyrin dimer** as a representative of a new class of phosphorus-containing porphyrins was synthesized. This structure exhibits remarkably broadened absorption as well as unique optoelectronic properties and is a good electron acceptor owing to the unique phosphole-fused structure.



### Porphyrinoids

T. Higashino,\* T. Yamada, T. Sakurai, S. Seki, H. Imahori\* — 12311–12315

Fusing Porphyrins and Phospholes: Synthesis and Analysis of a Phosphorus-Containing Porphyrin



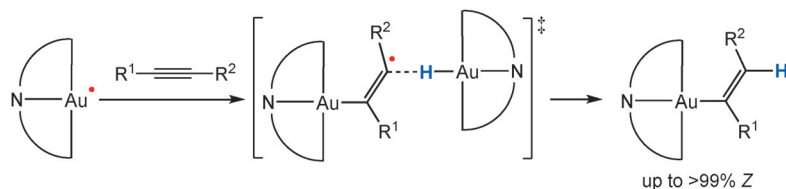
**Activation and functionalization of  $\text{N}_2$ :** A mixed diimide/dinitride tetranuclear titanium complex formed by activation of dinitrogen served as a unique platform for the synthesis of nitriles (see picture).

Functional groups such as aromatic C–X (X = Cl, Br, I) bonds, nitro groups, and ammonia-sensitive aldehyde and chloromethyl moieties were compatible with the synthetic method.

### Nitrogen Fixation

M. M. Guru, T. Shima, Z. Hou\* — 12316–12320

Conversion of Dinitrogen to Nitriles at a Multinuclear Titanium Framework



**Gold(II) provides a helping hand:** Gold(III) pincer complexes overcome their lack of substrate binding sites by participating in a radical-mediated bimolecular pathway. Gold(III) hydrides react with acety-

lenes in the presence of a radical source in a kinetically controlled reaction to give *trans*-hydroauration products with high regio- and stereoselectivity.

### Reaction Mechanisms

A. Pintus, L. Rocchigiani, J. Fernandez-Cestau, P. H. M. Budzelaar,\* M. Bochmann\* — 12321–12324

Stereo- and Regioselective Alkyne Hydrometallation with Gold(III) Hydrides

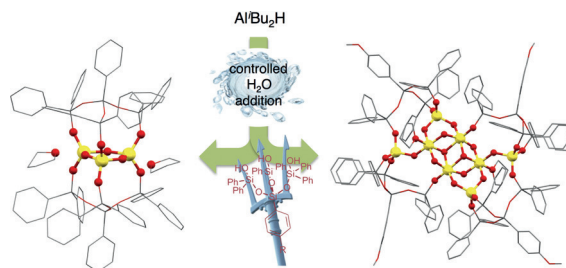


**Aluminate Models**

K. S. Lokare, N. Frank, B. Braun-Cula,  
I. Goikoetxea, J. Sauer,  
C. Limberg\* — 12325 – 12329



Trapping Aluminum Hydroxide Clusters  
with Trisilanols during Speciation in  
Aluminum(III)–Water Systems:  
Reproducible, Large Scale Access to  
Molecular Aluminate Models

**Inside Cover**

**Picking out early aggregates:** Tripodal trisilanols stabilize aluminum hydroxide aggregates formed during the hydrolysis

of  $\text{Al}(\text{Bu}_2\text{H})_3$  with different sizes dependent on the amount of water added.

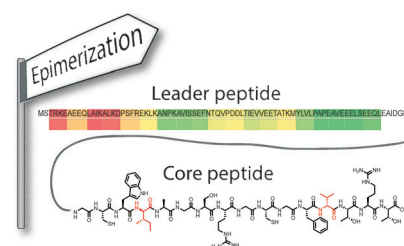
**Epimerases**

S. W. Fuchs, G. Lackner, B. I. Morinaka,  
Y. Morishita, T. Asai, S. Riniker,  
J. Piel\* — 12330 – 12333



A Lanthipeptide-like N-Terminal Leader  
Region Guides Peptide Epimerization by  
Radical SAM Epimerases: Implications for  
RiPP Evolution

**To guide an epimerase:** Radical S-adenosyl-methionine peptide epimerases from proteusin biosynthetic pathways introduce D-amino acids into ribosomal peptides. A region in proteusin peptide precursors is identified that is important for epimerization. This region and other shared features in precursors of proteusins, lanthipeptides, and other peptide classes suggest a common evolutionary origin with nitrile hydratase-like enzymes as ancestors.

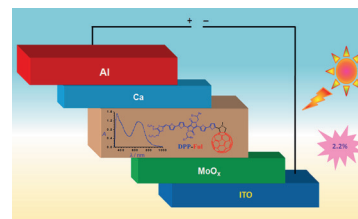
**Solar Cells**

K. Narayanaswamy, A. Venkateswararao,  
P. Nagarjuna, S. Bishnoi, V. Gupta,  
S. Chand, S. P. Singh\* — 12334 – 12337



An Organic Dyad Composed of Diathiafulvalene-Functionalized Diketopyrrolopyrrole–Fullerene for Single-Component High-Efficiency Organic Solar Cells

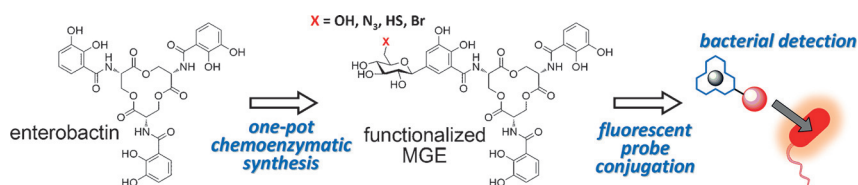
**Climbing alone:** The combination of dithiafulvalene-functionalized diketopyrrolopyrrole (DPP) as donor with fullerene (Ful) as acceptor has been successfully explored. Its utilization in single-component organic solar cells (SC-OSCs) was investigated, and it was shown to have a record power-conversion efficiency. ITO = indium tin oxide.

**Siderophore Conjugates**

A. A. Lee, Y.-C. S. Chen, E. Ekalestari,  
S.-Y. Ho, N.-S. Hsu, T.-F. Kuo,  
T.-S. A. Wang\* — 12338 – 12342

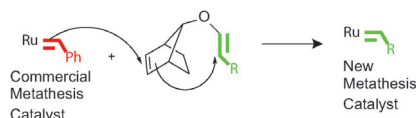


Facile and Versatile Chemoenzymatic  
Synthesis of Enterobactin Analogues and  
Applications in Bacterial Detection



**Siderophore-based bacteria labeling:** A one-pot chemoenzymatic synthesis approach that is capable of functionalizing enterobactin with different reactive groups is developed. The functionalized

enterobactin can be further conjugated with fluorophores to perform specific detection of bacteria. This strategy can serve as a convenient way to deliver cargos into bacteria with selectivity.

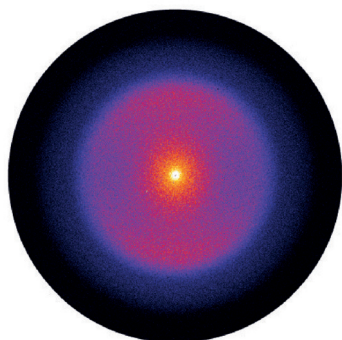
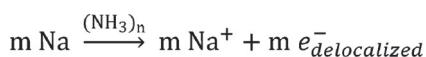


The preferred reaction of a commercial ruthenium benzylidene complex with a highly strained norbornene, followed by a fast intramolecular cyclization, yields new ruthenium carbene complexes in excellent yields. These complexes are ready for functional initiation of polymerization reactions without the need of purification.

### Olefin Metathesis

A. A. Nagarkar, M. Yasir, A. Crochet, K. M. Fromm, A. F. M. Kilbinger\* 12343–12346

Tandem Ring-Opening–Ring-Closing Metathesis for Functional Metathesis Catalysts

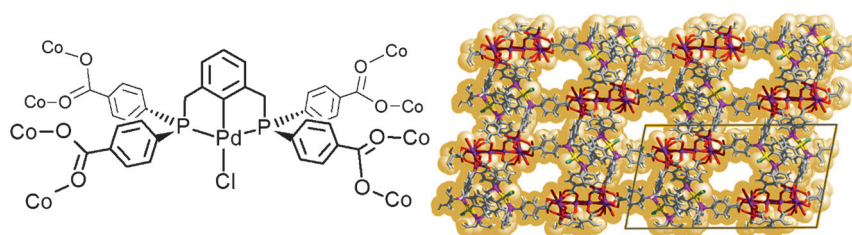


When is a metal not a metal? For more than a century, chemists have been struggling for a detailed understanding of the intriguing concentration-dependent color change of metal–ammonia solutions from deep blue to copper-gold. Indications for the underlying nonmetal-to-metal transition have now been found in photoelectron images of sodium–ammonia nanodroplets, paving the way for an atomistic description.

### Metal–Ammonia Solutions

S. Hartweg, A. H. C. West, B. L. Yoder, R. Signorell\* 12347–12350

Metal Transition in Sodium–Ammonia Nanodroplets



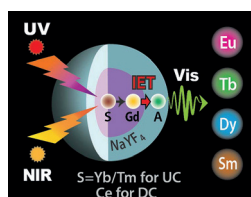
**Poly-PCP-pincers:** A new synthetic strategy for the formation of crystalline, porous versions of PCP-pincer complexes is presented. These complexes can selectively

activate gas molecules, such as CO<sub>2</sub> over CO, in the solid state. PCP = Porous Coordination Polymer

### Coordination Polymers

J. He, N. W. Waggoner, S. G. Dunning, A. Steiner, V. M. Lynch, S. M. Humphrey\* 12351–12355

A PCP Pincer Ligand for Coordination Polymers with Versatile Chemical Reactivity: Selective Activation of CO<sub>2</sub> Gas over CO Gas in the Solid State



**Up, down, flying around:** Photon up- and down-conversion (UC and DC, respectively) have been realized through Gd<sup>3+</sup>-mediated interfacial energy transfer (IET) in a core–shell nanoarchitecture. This finding offers a simple, efficient approach for photon management, and enables a fundamental understanding of the interactions between lanthanide ions at nanometer length scale.

### Up- and Down-Conversion

B. Zhou,\* L. Tao, Y. Chai, S. P. Lau, Q. Y. Zhang,\* Y. H. Tsang\* 12356–12360

Constructing Interfacial Energy Transfer for Photon Up- and Down-Conversion from Lanthanides in a Core–Shell Nanostructure



Inside Back Cover

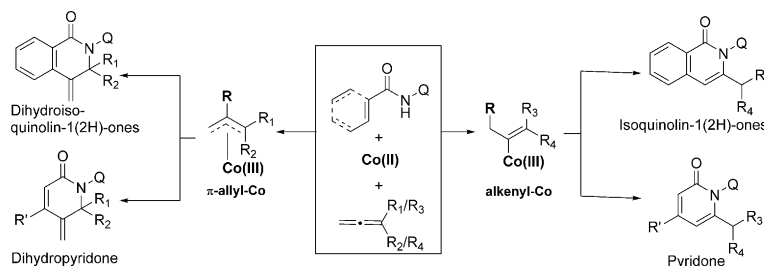


## C–H Activation

N. Thrimurtulu,\* A. Dey, D. Maiti,\*  
C. M. R. Volla\* — 12361 – 12365



Cobalt-Catalyzed  $sp^2$ -C–H Activation:  
Intermolecular Heterocyclization with  
Allenes at Room Temperature



**Two paths to ring formation:** Heterocyclization reactions of aryl and alkenylamides with allenes at room temperature are reported. The reactions, which involve

C–H activation using a Co catalyst, feature a high regioselectivity and impressive substrate scope for both coupling partners.

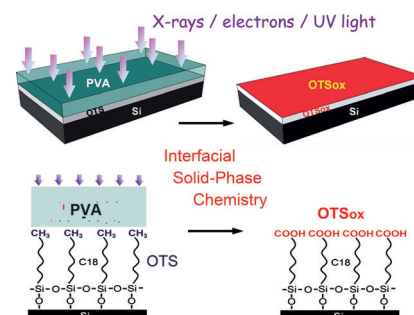
## Surface Functionalization

R. Maoz,\* D. Burshtain, H. Cohen,  
P. Nelson, J. Berson, A. Yoffe,  
J. Sagiv\* — 12366 – 12371



Site-Targeted Interfacial Solid-Phase  
Chemistry: Surface Functionalization of  
Organic Monolayers via Chemical  
Transformations Locally Induced at the  
Boundary between Two Solids

**Novel interfacial chemistry** is induced by electromagnetic radiation or electrons at the boundary between two solid materials, one of which acts as a removable thin film reagent/catalyst. This approach offers a variety of viable routes for nondestructive surface functionalization and patterning over length scales extending from centimeters to nanometers.

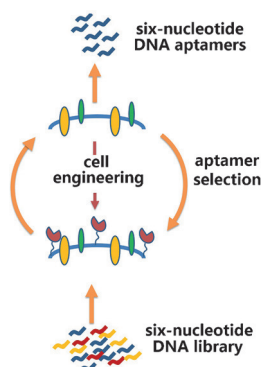


## Laboratory Evolution

L. Zhang, Z. Yang, T. L. Trinh, I. T. Teng,  
S. Wang, K. M. Bradley, S. Hoshika,  
Q. Wu, S. Cansiz, D. J. Rowold,  
C. McLendon, M. S. Kim, Y. Wu, C. Cui,  
Y. Liu, W. Hou, K. Stewart, S. Wan, C. Liu,\*  
S. A. Benner,\* W. Tan\* — 12372 – 12375



Aptamers against Cells Overexpressing  
Glypican 3 from Expanded Genetic  
Systems Combined with Cell Engineering  
and Laboratory Evolution



**Six nucleobases:** An expanded genetic information system and laboratory in vitro evolution were used to generate six-nucleotide aptamers that target cells engineered to overexpress a particular cell-surface protein. These aptamers could be used to distinguish cells that display that protein from those that do not.

## Peptides

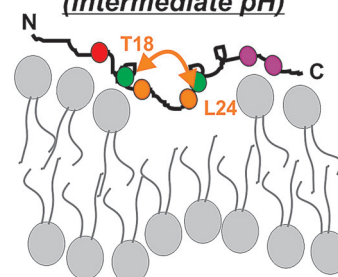
S. Z. Hanz, N. S. Shu, J. Qian,  
N. Christman, P. Kranz, M. An, C. Grever,  
W. Qiang\* — 12376 – 12381



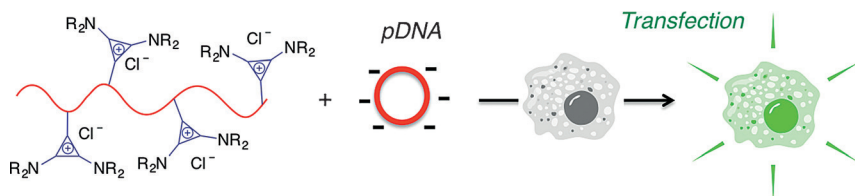
Protonation-Driven Membrane Insertion  
of a pH-Low Insertion Peptide

**Showing backbone:** The pH-low insertion peptide (pHLIP) inserts into membranes and forms a transmembrane (TM)  $\alpha$ -helix in response to acidity changes. Tracing backbone conformations revealed that the TM helix spans from A10 to D33 with a break at T19 to P20. Residue-specific  $pK_a$  values of D31, D33, D25, and D14 were determined to be 6.5, 6.3, 6.1, and 5.8, respectively, and define the sequence of protonations which lead to insertion. Furthermore, possible intermediate states which disrupt membranes at pH 6.4 are proposed.

**kinked conformation  
and membrane disruption  
(intermediate pH)**







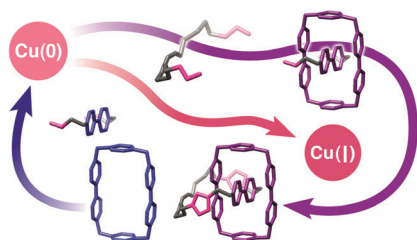
**They just clicked:** A stable bis(dialkylamino)cyclopropenium chloride salt can efficiently react with polymers containing secondary amines to yield cationic polyelectrolytes. The dialkylamino groups in this click transformation can be modu-

lated to yield various polyelectrolytes bearing soft cationic moieties. Some of these cyclopropenium-based polymers give high transfection efficiencies and are less cytotoxic than linear polyethyleneimine (PEI).

### Polymer Chemistry

J. L. Freyer, S. D. Brucks, G. S. Gobieski, S. T. Russell, C. E. Yozwiak, M. Sun, Z. Chen, Y. Jiang, J. S. Bandar, B. R. Stockwell, T. H. Lambert,\*  
L. M. Campos\* ————— 12382 – 12386

Clickable Poly(ionic liquids): A Materials Platform for Transfection

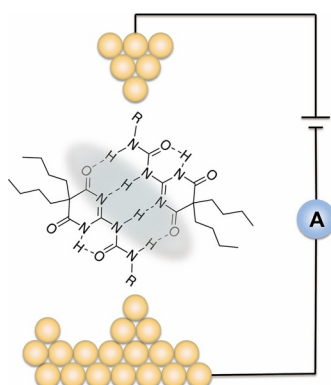


**A user-friendly technique** for the construction of positively charged catenanes and rotaxanes, templated by radical-pairing interactions in a convenient and efficient manner, has been conceived and implemented. This method opens up the possibility of producing integrated systems with Coulombically challenged catenanes and rotaxanes and of fabricating devices based on these systems.

### Supramolecular Chemistry

Y. Wang, J. Sun, Z. Liu, M. S. Nassar, Y. Y. Botros,  
J. F. Stoddart\* ————— 12387 – 12392

Symbiotic Control in Mechanical Bond Formation

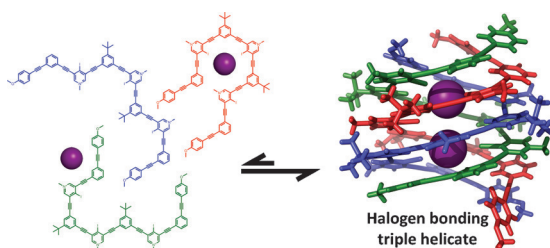


**Electron transport through multiple hydrogen bonds:** Supramolecular junctions bridged with quadruple hydrogen bonds have been constructed and characterized using the scanning tunneling microscopy break junction method. This noncovalent interaction exhibits conductivity comparable to that of covalently conjugated molecular devices and can also be manipulated by the polarity of the solvent environment.

### Molecular Electronics

L. Wang, Z.-L. Gong, S.-Y. Li, W. Hong,\*  
Y.-W. Zhong,\* D. Wang,\*  
L.-J. Wan ————— 12393 – 12397

Molecular Conductance through a Quadruple-Hydrogen-Bond-Bridged Supramolecular Junction



**Bond, halogen bond:** Three tricationic arylethynyl strands self-assemble to form a tubular anion channel lined with nine halogen-bond donors in solution and the solid state. Eight strong iodine...iodide halogen bonds and numerous buried

$\pi$ -surfaces endow the triplex with remarkable stability, even at elevated temperatures. The stringent linearity of halogen bonding could be a powerful tool for the synthesis of multi-strand anion helicates.

### Supramolecular Chemistry

C. J. Massena, N. B. Wageling,  
D. A. Decato, E. Martin Rodriguez,  
A. M. Rose,  
O. B. Berryman\* ————— 12398 – 12402

A Halogen-Bond-Induced Triple Helicate Encapsulates Iodide



Front Cover



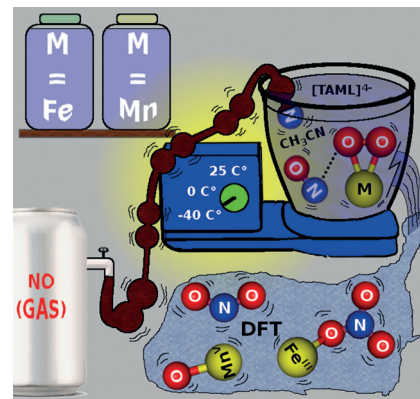
## Nitric Oxide Chemistry

S. Hong, P. Kumar, K.-B. Cho, Y.-M. Lee,  
K. D. Karlin,\* W. Nam\* — 12403 – 12407



Mechanistic Insight into the Nitric Oxide  
Dioxygenation Reaction of Nonheme  
Iron(III)–Superoxo and Manganese(IV)–  
Peroxo Complexes

**By NO means:** Reactions of nonheme  
 $\text{Fe}^{\text{III}}$ –superoxo and  $\text{Mn}^{\text{IV}}$ –peroxo com-  
plexes bearing a common tetraamido  
macrocyclic ligand (TAML), namely  
 $[(\text{TAML})\text{Fe}^{\text{III}}(\text{O}_2)]^{2-}$  and  $[(\text{TAML})\text{Mn}^{\text{IV}}(\text{O}_2)]^{2-}$ , with nitric oxide (NO) afford the  
 $\text{Fe}^{\text{III}}$ – $\text{NO}_3$  complex  $[(\text{TAML})\text{Fe}^{\text{III}}(\text{NO}_3)]^{2-}$   
and the  $\text{Mn}^{\text{V}}$ –oxo complex  $[(\text{TAML})\text{Mn}^{\text{V}}(\text{O})]^{+}$  plus  $\text{NO}_2^{-}$ , respectively.



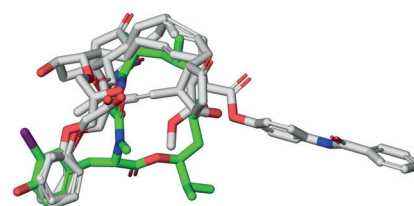
## Natural Products

G. Schneider,\* D. Reker, T. Chen,  
K. Hauenstein, P. Schneider,  
K.-H. Altmann — 12408 – 12411



Deorphaning the Macromolecular Targets  
of the Natural Anticancer Compound  
Doliculide

**Computational adoption services:** Macro-  
molecular targets of the marine natural  
product doliculide were successfully  
identified using a chemocentric com-  
puter-based prediction method. This  
study reveals this cyclodepsipeptide as  
a potent antagonist of the human pros-  
tanoic acid receptor EP3.



## Pressure and Temperature

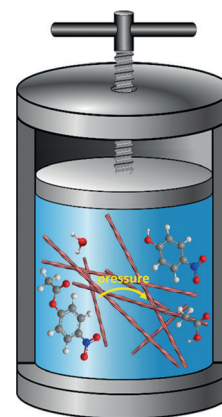
T. Q. Luong, N. Erwin, M. Neumann,  
A. Schmidt, C. Loos, V. Schmidt,  
M. Fändrich,\* R. Winter\* — 12412 – 12416



Hydrostatic Pressure Increases the  
Catalytic Activity of Amyloid Fibril  
Enzymes

## Negative + positive = better catalysis:

Studying the combined effects of pressure  
and temperature on the hydrolysis of *p*-  
nitrophenyl acetate catalyzed by designed  
amyloid fibrils using high-pressure  
stopped-flow techniques with rapid UV/  
Vis absorbance detection showed that  
both pressure and temperature effectively  
enhance the catalysis as a consequence of  
a negative activation volume and a pos-  
itive activation energy.

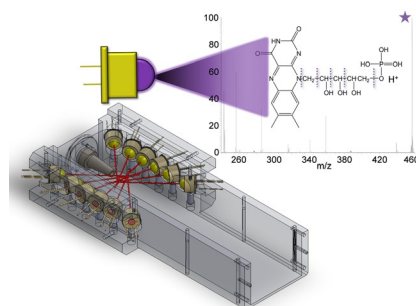


## Analytical Chemistry

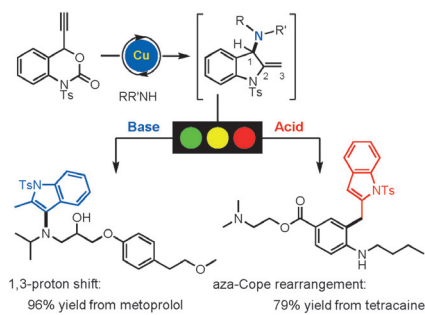
D. D. Holden, A. Makarov, J. C. Schwartz,  
J. D. Sanders, E. Zhuk,  
J. S. Brodbelt\* — 12417 – 12421



Ultraviolet Photodissociation Induced by  
Light-Emitting Diodes in a Planar Ion Trap



**LEDs as an ultraviolet photodissociation  
light source:** The latest ultraviolet LEDs  
are interfaced with a mass spectrometer  
to perform gas-phase ultraviolet photo-  
dissociation of cations and anions.

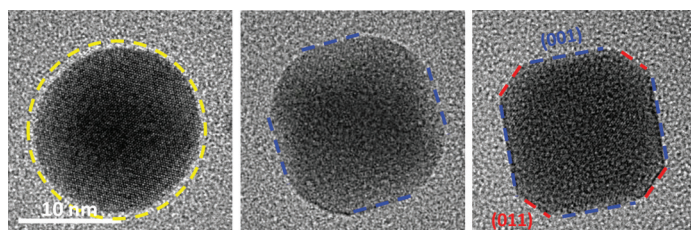


**Switch-hitter:** This work describes a copper-catalyzed decarboxylative amination/hydroamination sequential reaction. The one-pot treatment of an indoline intermediate with either an acid or a base enables the switchable synthesis of two types of functionalized indoles in generally high yields and with complete chemoselectivities (36 examples and up to 99% yield).

## Heterocycles

T.-R. Li, B.-Y. Cheng, Y.-N. Wang,  
M.-M. Zhang, L.-Q. Lu,\*  
W.-J. Xiao 12422 – 12426

A Copper-Catalyzed Decarboxylative Amination/Hydroamination Sequence: Switchable Synthesis of Functionalized Indoles



**In good shape:** Deliberate surface faceting of palladium–copper alloyed nanocrystals was achieved by simple post-synthetic treatment in atmospheric

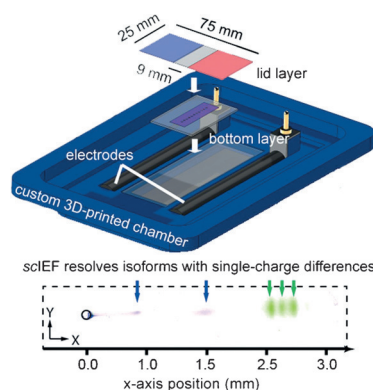
pressure hydrogen. Microscopic insight is provided for tailoring of the physical and chemical properties of catalytically significant palladium alloys.

## Nanoparticle Morphology

Y. Jiang, H. Li, Z. Wu, W. Ye, H. Zhang,  
Y. Wang,\* C. Sun,\*  
Z. Zhang 12427 – 12430

In Situ Observation of Hydrogen-Induced Surface Faceting for Palladium–Copper Nanocrystals at Atmospheric Pressure

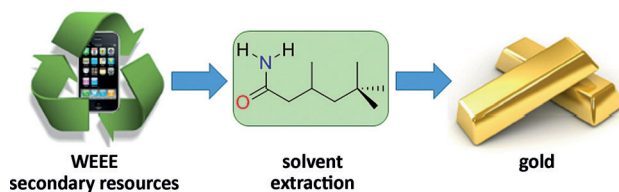
**Electrophoretic cytometry:** A multilayer, patterned hydrogel device supports isoelectric focusing to separate protein isoforms from single cells (scIEF). All preparative and analytical steps, including cell isolation, lysis, protein separation, UV-actuated blotting, and immunoprobing, are performed on the device. Protein isoforms with single-charge differences are resolved, blotted, and detected by immunoprobing.



## Single-Cell Analysis

A. M. Tentori, K. A. Yamauchi,  
A. E. Herr\* 12431 – 12435

Detection of Isoforms Differing by a Single Charge Unit in Individual Cells



**Going for gold:** A simple primary amide is shown to be an effective reagent for the selective recovery of gold by solvent extraction from a mixture of metals representative of those in waste electrical and

electronic equipment (WEEE). The recovery is achieved through the formation of dynamically assembled hydrogen-bonded amide/AuCl<sub>4</sub> clusters.

## Recovery of Gold

E. D. Doidge, I. Carson, P. A. Tasker,  
R. J. Ellis, C. A. Morrison,  
J. B. Love\* 12436 – 12439

A Simple Primary Amide for the Selective Recovery of Gold from Secondary Resources



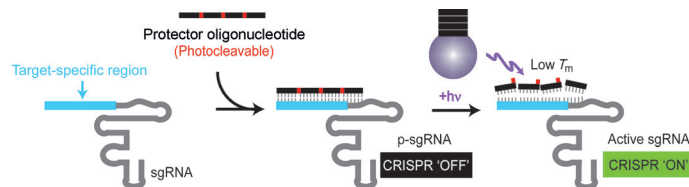


## Gene Technology

P. K. Jain, V. Ramanan, A. G. Schepers,  
N. S. Dalvie, A. Panda, H. E. Fleming,  
S. N. Bhatia\* ————— 12440 – 12444



Development of Light-Activated CRISPR  
Using Guide RNAs with Photocleavable  
Protectors



**Turn “ON” CRISPR with light:** CRISPR can be brought under the control of light simply by hybridizing a single chimeric guide RNA (sgRNA) with a complementary oligonucleotide containing photo-

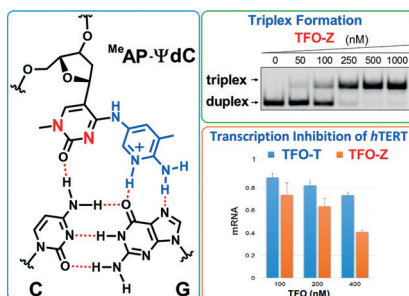
cleavable groups (protector oligonucleotide). The protected sgRNA (p-sgRNA) remains inactive, blocking CRISPR activity, until the protector oligonucleotide is cleaved with a remote light trigger.

## DNA Recognition

H. Okamura, Y. Taniguchi,\*  
S. Sasaki\* ————— 12445 – 12449



Aminopyridinyl-Pseudodeoxycytidine  
Derivatives Selectively Stabilize Anti-  
parallel Triplex DNA with Multiple CG  
Inversion Sites



**Pseudo-deoxycytidine (ΨdC) derivatives** were developed for the selective recognition of the CG base pair to expand the triplex-forming sequence. The ΨdCs formed a stable triplex with the promoter of the hTERT gene containing four CG inversion sites, and effectively inhibited its transcription in human cancer cells, and may lead to the development of new triplex-forming oligonucleotides.

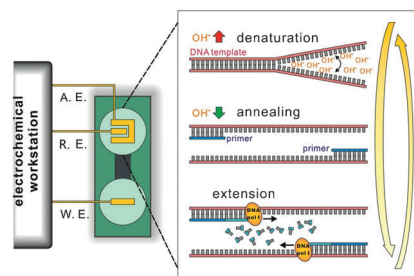
## DNA Replication

Y. Zhang, Q. Li, L. Guo, Q. Huang, J. Shi,  
Y. Yang, D. Liu,\* C. Fan\* — 12450 – 12454



Ion-Mediated Polymerase Chain  
Reactions Performed with an  
Electronically Driven Microfluidic Device

**A pH-legmatic approach to PCR:** Polymerase chain reactions were triggered at room temperature by using automatic pH alternation with a microfabricated device.



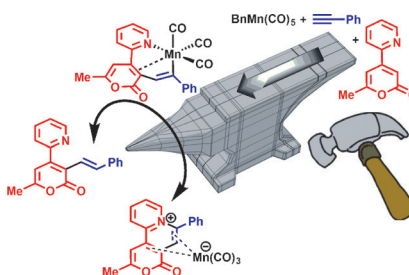
## C–H Activation



N. P. Yahaya, K. M. Appleby, M. Teh,  
C. Wagner, E. Troschke, J. T. W. Bray,  
S. B. Duckett, L. A. Hammarback,  
J. S. Ward, J. Milani, N. E. Pridmore,  
A. C. Whitwood, J. M. Lynam,\*  
I. J. S. Fairlamb\* ————— 12455 – 12459

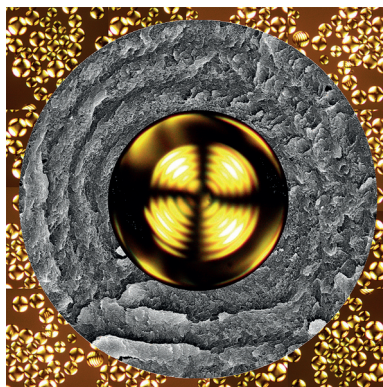


Manganese(I)-Catalyzed C–H Activation:  
The Key Role of a 7-Membered  
Manganacycle in H-Transfer and  
Reductive Elimination



**Look left, look right:** A highly reactive seven-membered manganese(I) intermediate has been detected and characterized that is effective for H-transfer or reductive elimination to deliver alkenylated or pyridinium products, respectively. The two pathways are determined at Mn<sup>I</sup> by judicious choice of an electron-deficient 2-pyrone substrate containing a 2-pyridyl directing group, which undergoes regioselective C–H activation.

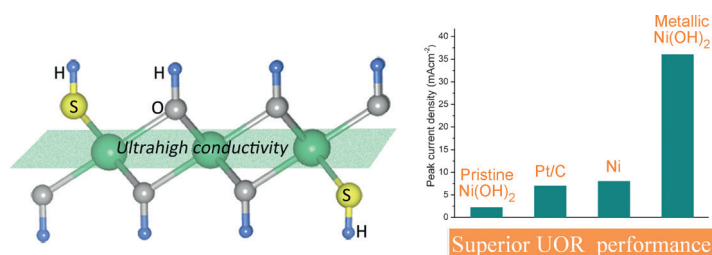
**Polymer microspheres** with chiral nematic order were obtained through photopolymerization of acrylamide in the presence of cellulose nanocrystals (CNCs). Using this approach, silica microspheres with chiral nematic structures were also fabricated for the first time.



### Polymer Microspheres

P.-X. Wang, W. Y. Hamad,  
M. J. MacLachlan\* — 12460 – 12464

Polymer and Mesoporous Silica Microspheres with Chiral Nematic Order from Cellulose Nanocrystals



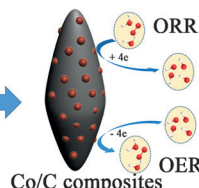
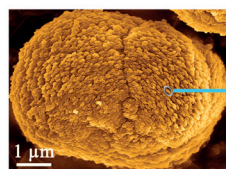
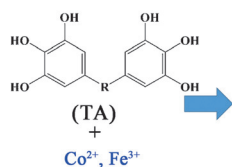
**Metal as anything:** Surface sulfur incorporation into  $\beta$ -Ni(OH)<sub>2</sub> nanosheets gives the first metallic configuration of a transition-metal hydroxide. The resulting metallic Ni(OH)<sub>2</sub> nanosheets have more

exposed active sites and metallic electrical conductivity, giving rise to greatly enhanced performance for the urea oxidation reaction (UOR) for direct urea fuel cells.

### Direct Urea Fuel Cells

X. J. Zhu, X. Y. Dou, J. Dai, X. D. An,  
Y. Q. Guo, L. D. Zhang, S. Tao, J. Y. Zhao,  
W. S. Chu, X. C. Zeng, C. Z. Wu,\*  
Y. Xie — 12465 – 12469

Metallic Nickel Hydroxide Nanosheets Give Superior Electrocatalytic Oxidation of Urea for Fuel Cells



**Coordination crystals** (see SEM image) obtained from a polyphenol (tannic acid; TA) and cobalt or iron were synthesized by a hydrothermal synthesis route. The crystals

are a renewable source for the fabrication of metal/carbon composites as a nonprecious metal catalyst for the oxygen reduction and evolution reactions.

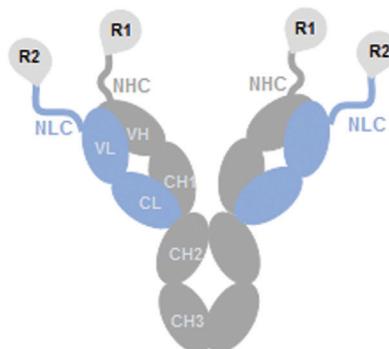
### Electrocatalysis

J. Wei, Y. Liang, Y. X. Hu, B. Kong,  
J. Zhang, Q. F. Gu, Y. P. Tong, X. B. Wang,  
S. P. Jiang, H. T. Wang\* — 12470 – 12474

Hydrothermal Synthesis of Metal–Polyphenol Coordination Crystals and Their Derived Metal/N-doped Carbon Composites for Oxygen Electrocatalysis



**Mono- and multifunctional antibody agonists** of the receptors GLP-1R, GCGR, and GIPR were generated by N-terminal fusion of the exendin-4, glucagon-like peptide-1, glucagon, GIP, and ZP peptides to the heavy chains (HC) and/or light chains (LC) of the humanized monoclonal antibody Synagis. The resulting antibody fusions show excellent activity in sustaining blood glucose control and reducing body weight in rodent models.



### Protein Engineering

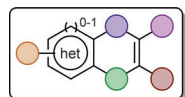
Y. Wang, J. Du, H. Zou, Y. Liu, Y. Zhang,  
J. Gonzalez, E. Chao, L. Lu, P. Yang,  
H. Parker, V. Nguyen-Tran, W. Shen,  
D. Wang, P. G. Schultz,\*  
F. Wang\* — 12475 – 12478

Multifunctional Antibody Agonists Targeting Glucagon-like Peptide-1, Glucagon, and Glucose-Dependent Insulinotropic Polypeptide Receptors

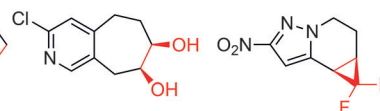


## Drug Discovery

D. G. Twigg, N. Kondo, S. L. Mitchell,  
W. R. J. D. Galloway, H. F. Sore, A. Madin,  
D. R. Spring\* 12479–12483



- 15 distinct scaffolds  
- 3–6 steps  
- divergent route



42 diverse examples  
35 with new chiral centres



Partially Saturated Bicyclic Hetero-  
aromatics as an  $sp^3$ -Enriched Fragment  
Collection

**2D or not 2D:** A collection of partially saturated bicyclic pyridine- and pyrazole-based fragments, derived from a diverse set of readily accessible branch-point scaffolds, is presented. Their enhanced

$sp^3$  content, compared to typical fragment libraries, allows excellent control of 3D growth vectors in drug development applications.

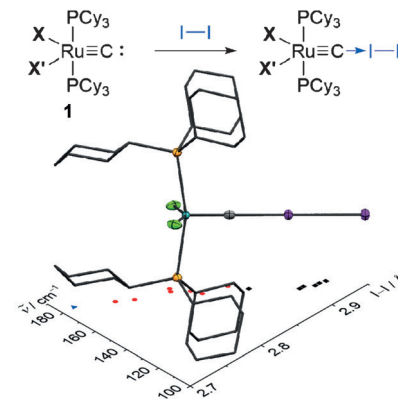
## Iodine Adducts

A. Reinholdt, T. Vosch,  
J. Bendix\* 12484–12487



Modification of  $\sigma$ -Donor Properties of  
Terminal Carbide Ligands Investigated  
Through Carbide–Iodine Adduct  
Formation

**To give and take:** terminal ruthenium carbide complexes  $[(C_3P)_2X_2Ru\equiv C]$  (**1**; X = halide or pseudohalide), form charge-transfer adducts with  $I_2$  exhibiting large variation in bond lengths and stretching frequencies. This shows that the auxiliary ligand sphere on ruthenium enables control over the  $\sigma$ -donor properties of carbide ligands, elucidating their isolobal relationship with carbon monoxide.



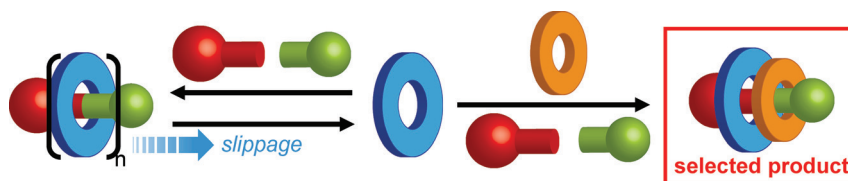
## Supramolecular Chemistry



E. A. Neal, S. M. Goldup\* 12488–12493



A Kinetic Self-Sorting Approach to  
Heterocircuit [3]Rotaxanes



**If at first you don't succeed, fall apart:** A novel self-sorting approach is described in which the kinetic stability of the desired [3]rotaxane isomer determines the reaction outcome. All other threaded struc-

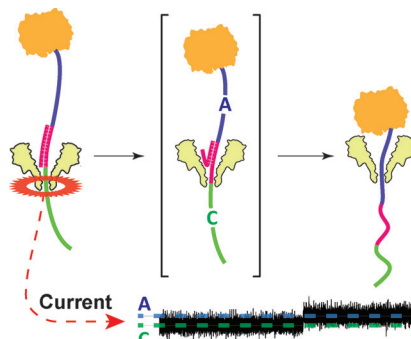
tures derived from the larger ring are kinetically unstable, allowing the yield of the target to be amplified at the expense of other possible products.

## Biosensors

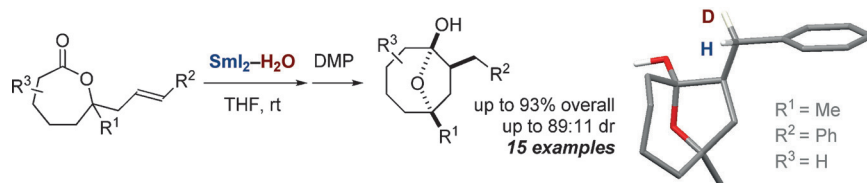
C. Wloka, N. L. Mutter, M. Soskine,\*  
G. Maglia\* 12494–12498



Alpha-Helical Fragaceatoxin C Nanopore  
Engineered for Double-Stranded and  
Single-Stranded Nucleic Acid Analysis



**A biological nanopore** with a deformable alpha-helical transmembrane region allows discrimination between homopolymeric single-stranded DNA and permits double-stranded DNA analysis.



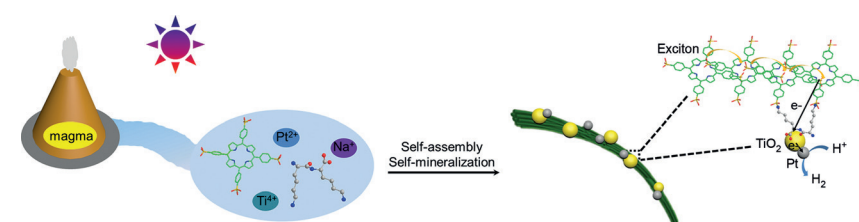
**Seven-membered lactones** undergo selective  $\text{SmI}_2\text{-H}_2\text{O}$ -promoted radical cyclization to form substituted cyclooctanols. The products arise from an *exo*-mode of cyclization rather than the usual *endo*-attack. A labeling experiment and

neutron diffraction study have been used for the first time to probe the configuration and highly diastereoselective deuteration of a chiral organosamarium intermediate.

### Radical Cyclization

X. Just-Baringo, J. Clark, M. J. Gutmann, D. J. Procter\* 12499–12502

Selective Synthesis of Cyclooctanoids by Radical Cyclization of Seven-Membered Lactones: Neutron Diffraction Study of the Stereoselective Deuteration of a Chiral Organosamarium Intermediate



**Mimicking primitive photosystems:** Self-organization, dynamic evolution, and sustainable utilization of components in a “prebiotic soup” are conceptually and experimentally validated through simple

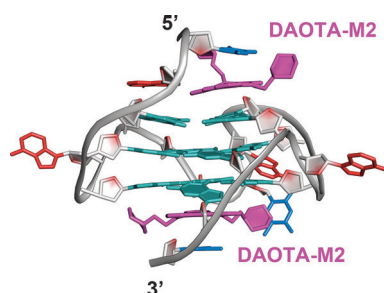
but well-functioning peptide–porphyrin co-assemblies, which support a new type of primitive hydrogen producing photobacteria model.

### Biomimetic Self-Organization

K. Liu, R. Xing, Y. Li, Q. Zou, H. Möhwald, X. Yan\* 12503–12507

Mimicking Primitive Photobacteria: Sustainable Hydrogen Evolution Based on Peptide–Porphyrin Co-Assemblies with a Self-Mineralized Reaction Center

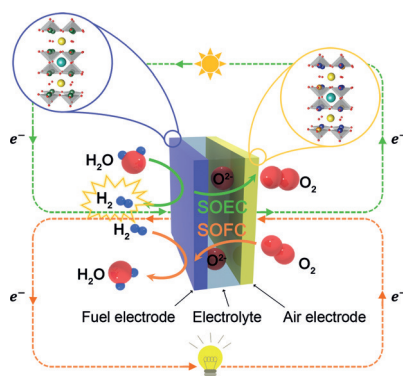
**Playing the triangle in a quartet:** A small-molecule optical probe (DAOTA-M2) based on a triangulenium core binds to G-quadruplexes in a 1:2 stoichiometry. Binding of DAOTA-M2 occurs mainly through  $\pi\text{-}\pi$  stacking between the triangulenium core and the guanine residues of the outer G-quartets. Interestingly, the binding affinities of DAOTA-M2 for the two outer G-quartets differ by a factor of two.



### G-Quadruplexes

A. Kotar, B. Wang, A. Shivalingam, J. Gonzalez-Garcia, R. Vilar, J. Plavec\* 12508–12511

NMR Structure of a Triangulenium-Based Long-Lived Fluorescence Probe Bound to a G-Quadruplex



**A solid oxide electrolysis cell** using layered perovskites as both-side electrodes is shown to possess outstanding performance, reversible cycling, and long-term stability during hydrogen production.

### Hydrogen Productions

A. Jun, J. Kim, J. Shin, G. Kim\* 12512–12515

Achieving High Efficiency and Eliminating Degradation in Solid Oxide Electrochemical Cells Using High Oxygen-Capacity Perovskite

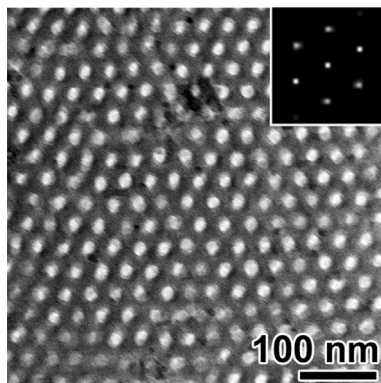


**Conducting Polymers**

S. Liu, J. Zhang, R. Dong, P. Gordiichuk,  
T. Zhang, X. Zhuang, Y. Mai, F. Liu,  
A. Herrmann, X. Feng\* — **12516–12521**



Two-Dimensional Mesoscale-Ordered  
Conducting Polymers



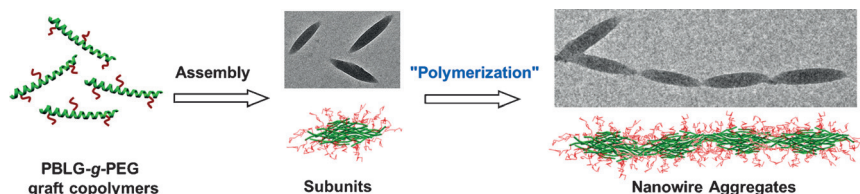
**Ultrathin conducting polymer nanosheets** were achieved by synergistically manipulating the self-assembly of perfluorocarboxylic acids and polystyrene-*b*-poly(ethylene oxide) diblock copolymers. The nanosheets feature mesoscale-ordered hexagonal pore arrays, tunable morphologies and pore sizes, large specific surface area as well as anisotropic and record-high electrical conductivity.

**Hierarchical Assembly**

Z. Zhuang, T. Jiang, J. Lin,\* L. Gao,  
C. Yang, L. Wang,\* C. Cai — **12522–12527**



Hierarchical Nanowires Synthesized by  
Supramolecular Stepwise Polymerization



**Connect the dots:** Anisotropic spindle-like micelles, self-assembled from polypeptide graft copolymers with rigid backbones, can serve as ideal pre-assembled subunits

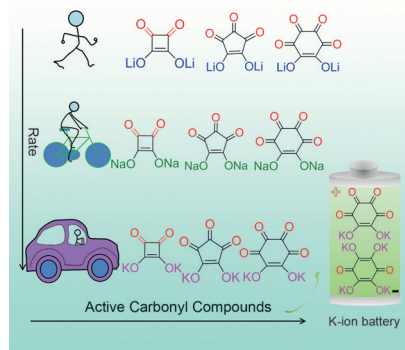
for constructing hierarchical nanowires. The growth of the nanowires follows a hierarchical process that resembles step polymerization.

**Energy Storage**

Q. Zhao, J. Wang, Y. Lu, Y. Li, G. Liang,  
J. Chen\* — **12528–12532**



Oxocarbon Salts for Fast Rechargeable  
Batteries



**Organic electrode material:** Oxocarbon salts ( $M_2(CO)_n$ ) with different metal ions ( $M = Li, Na, K$ ) and frameworks ( $n = 4, 5, 6$ ) were rationally designed and used as electrodes for rechargeable Li, Na, and K-ion batteries. A first example of a renewable and sustainable K-ion battery based on  $K_2C_6O_6$  and  $K_4C_6O_6$  with a rocking-chair reaction mechanism is shown.

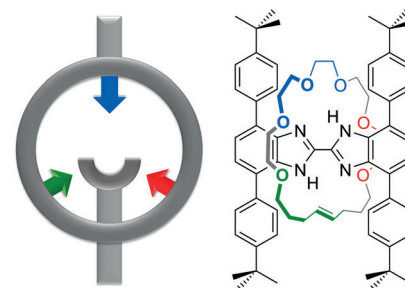
**Supramolecular Chemistry**

G. Baggi, S. J. Loeb\* — **12533–12537**

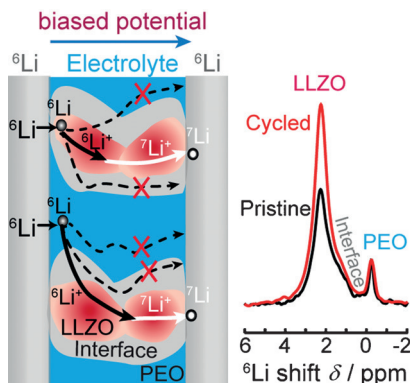


Rotationally Active Ligands: Dialing-Up  
the Co-conformations of a [2]Rotaxane for  
Metal Ion Binding

A rigid, H-shaped [2]rotaxane ligand with different sets of donor atoms on the axle and wheel components was prepared. The dynamics of the rotaxane and the orthogonal arrangement of the donors allows access to different co-conformations by simple rotation of the wheel about the axle. Three different rotational isomers were observed and structurally characterized for the neutral ligand and coordination complexes with  $Li^+$  and  $Cu^+$  ions.



**Where do they go?** The first experimental evidence was obtained for lithium ions diffusing through composite ceramic electrolytes (LLZO and PEO) in an all-solid-state battery. Lithium ion diffusion was determined using  $^6,7\text{Li}$  NMR and isotope exchange, and indicated that Li ions mainly pass through the LLZO-PEO ceramic phase instead of the LLZO-PEO interface or the PEO phase.



## Batteries

J. Zheng, M. Tang,  
Y.-Y. Hu\* 12538–12542

Lithium Ion Pathway within  $\text{Li}_7\text{La}_3\text{Zr}_2\text{O}_{12}$ -  
Polyethylene Oxide Composite  
Electrolytes



Supporting information is available on [www.angewandte.org](http://www.angewandte.org) (see article for access details).



A video clip is available as Supporting Information on [www.angewandte.org](http://www.angewandte.org) (see article for access details).



This article is available online free of charge (Open Access).



This article is accompanied by a cover picture (front or back cover, and inside or outside).

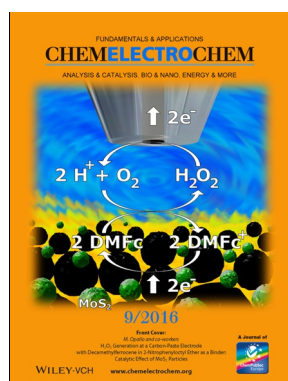


The Very Important Papers, marked VIP, have been rated unanimously as very important by the referees.

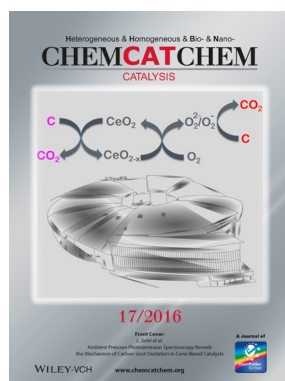


The Hot Papers are articles that the Editors have chosen on the basis of the referee reports to be of particular importance for an intensely studied area of research.

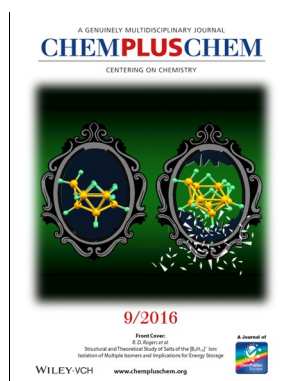
## Check out these journals:



[www.chemelectrochem.org](http://www.chemelectrochem.org)



[www.chemcatcher.org](http://www.chemcatcher.org)



[www.chempluschem.org](http://www.chempluschem.org)



[www.chemviews.org](http://www.chemviews.org)

Angewandte  
Corrigendum

Substrate-Controlled Product  
Divergence: Conversion of CO<sub>2</sub> into  
Heterocyclic Products

J. Rintjema, R. Epping, G. Fiorani,  
E. Martín, E. C. Escudero-Adán,  
A. W. Kleij\* 3972–3976

Angew. Chem. Int. Ed. 2016, 55

DOI: 10.1002/anie.201511521

Figure 2 of this Communication needs to be revised as shown below. Specifically, compounds **18** and **19** were erroneously exchanged from their position. The authors wish to apologize for this error.

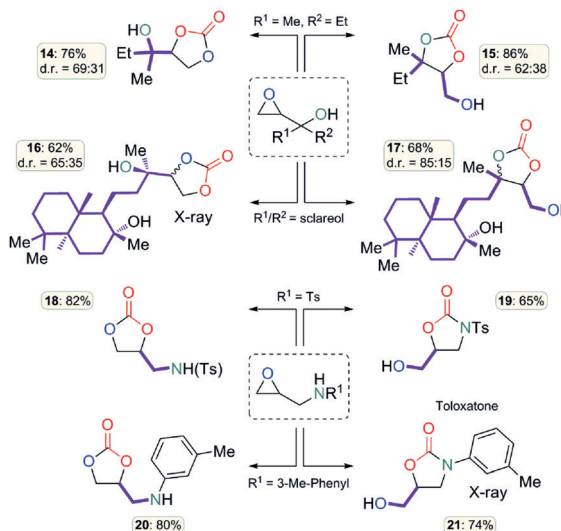


**Figure 2.** Product divergence from four epoxy alcohols/amines, thus giving access to the compounds **14–21**. For all reactions 2 mol % [Al<sup>tBu</sup>] and  $p(\text{CO}_2)^\circ = 10$  bar were used unless indicated otherwise. Details: **14**, 5 mol % TBAB, 25 °C, 60 h, conv. 95%, sel. 85%; **15**, 80 °C, 40 h, 30 bar, conv. > 99%, sel. 93%; **16**, 5 mol % TBAB, 50 °C, 14 h, 30 bar, conv. > 99%, sel. 79%; **17**, 10 mol % TBACl, 75 °C, 14 h, conv. > 99%, sel. 79%; **18**, 5 mol % TBAB, 75 °C, 14 h, conv. > 99%, sel. 97%; **19**, 10 mol % DIPEA, 50 °C, 40 h, 30 bar, conv. > 99%, sel. 77%; **20**, 5 mol % TBAB, 30 °C, 40 h, conv. > 99%, sel. 81%; **21**, 2 mol % TBAB, 75 °C, 14 h, conv. > 99%, sel. 81%.<sup>[13]</sup> Ts = 4-toluenesulfonyl.

Angewandte  
Corrigendum

Benzimidazobenzothiazole-based  
Bipolar Hosts to Harvest Nearly All of the  
Excitons from Blue Delayed Fluorescence  
and Phosphorescent Organic Light-  
Emitting Diodes

L.-S. Cui, J. U. Kim, H. Nomura,  
H. Nakanotani, C. Adachi\* 6864–6868

Angew. Chem. Int. Ed. 2016, 55

DOI: 10.1002/anie.201601136

The authors of this Communication wish to cite an additional contribution. For this reason, reference [13] must be added on page 6864, right column, at the end of the second sentence of the second paragraph: “The benzimidazo[2,1-*b*]benzothiazole backbone was synthesized through cyclization of 2-mercaptobenzimidazole with *o*-nitrophenyl bromide.<sup>[13]</sup>”

[13] The synthesis of benzimidazobenzothiazole backbone was reported by Lv et al. and Schäfer et al.: a) J. Gao, J. Zhu, L. Chen, Y. Shao, J. Zhu, Y. Huang, X. Wang, X. Lv, *Tetrahedron Lett.* **2014**, 55, 3367; b) T. Schäfer, P. Murer, U. Heinemeyer, J. Kohlstedt, H. Wolleb, A. Wolleb, S. Watanabe, H. Nagashima, T. Sakai, C. Lennartz, G. Wagenblast, Patent WO, 2015014794, 2015.